arXiv:cond-mat/0106599v1 [cond-mat.str-el] 28 Jun 2001

The Cerium volume collapse: Results from the LDA+DMFT approach

K. Held,[1] A.K. McMahan,[2] and R.T. Scalettar[3]
[1]*Physics Department, Princeton University, Princeton, NJ 08544*
[2]*Lawrence Livermore National Laboratory, University of California, Livermore, CA 94550*
[3]*Physics Department, University of California, Davis, CA 95616*
(February 1, 2008)

The merger of density-functional theory in the local density approximation (LDA) and many-body dynamical mean field theory (DMFT) allows for an *ab initio* calculation of Ce including the inherent $4f$ electronic correlations. We solve the DMFT equations by the quantum Monte Carlo (QMC) technique and calculate the Ce energy, spectrum, and double occupancy as a function of volume. At low temperatures, the correlation energy exhibits an anomalous region of negative curvature which drives the system towards a thermodynamic instability, i.e., the γ-to-α volume collapse, consistent with experiment. The connection of the energetic with the spectral evolution shows that the physical origin of the energy anomaly and, thus, the volume collapse is the appearance of a quasiparticle resonance in the $4f$-spectrum which is accompanied by a rapid growth in the double occupancy.

PACS numbers: 71.27.+a, 71.20.Eh, 75.20.Hr

Cerium exhibits the well known γ-α phase transition characterized by an unusually large volume change of 15% [1]. Similar volume collapse transitions are observed under pressure in Pr and Gd (for a recent review see [2]). It is widely believed that these transitions arise from changes in the degree of $4f$ electron correlation, as is reflected in both the Kondo volume collapse [3] and the Mott transition [4] models. The former ascribes the collapse to a rapid change in the valence-electron screening of the local $4f$-moment, which is accompanied by the appearance of an Abrikosov-Suhl-like quasiparticle peak at the Fermi level, lying between the remaining Hubbard-split $4f$ spectral density. In other words, the Kondo temperature of the α-phase is much larger than that of the γ-phase. While originally formulated in terms of the Anderson impurity model, similar rapid thermodynamic and spectral changes are seen for the lattice version, or periodic Anderson model [5].

The Mott transition model envisions a more abrupt change from itinerant, bonding character of the $4f$-electrons in the α-phase to non-bonding, localized character in the γ-phase, driven by changes in the $4f$-$4f$ intersite hybridization. Thus, as the ratio of the $4f$ Coulomb interaction to the $4f$-bandwidth increases with increasing volume, a Mott transition occurs to the γ-phase. While originally motivated by the Hubbard model, most recent support for this perspective has come from orbitally polarized [6] and self-interaction corrected [7] modifications of local-density functional theory. It has been argued [2] that these modified local-density methods resemble static mean field treatments in which the γ-phase is spin and orbitally polarized such that the 14 $4f$-bands are Hubbard split into one band below and 13 above the Fermi level for Ce. At smaller volumes, the mean-field polarization disappears and, thus, the α-phase resembles the ordinary LDA solution with all 14 bands grouped together just above but slightly overlapping the Fermi level. While this approach gives the correct energy in the limit of small volume, and also at low temperature for large volume (though not the correct paramagnetic phase), a true many-body solution would allow for a central quasiparticle peak in the presence of the Hubbard splitting as observed in the Mott transition of the one-band Hubbard model [8,9]. The Kondo volume collapse calculations [3], on the other hand, take such electronic correlations into account but are based on simplified models.

In this situation, the recently developed merger [10] of LDA [11] and DMFT [12,8] offers an ideal means to study Ce realistically, including the critical intrasite $4f$ electron correlations [13]. Only two very recent LDA+DMFT calculations have been reported to date for f-electron systems. Savrasov, Kotliar, and Abrahams [14] have employed an interpolation scheme to the DMFT self-energy inspired by the iterative perturbation theory (IPT), and present total energy calculations and the spectrum for Pu. Zölfl *et al.* [15] have used the non-crossing approximation (NCA) to report the first Ce α- and γ-phase spectra. Both papers find Hubbard splitting, with an additional quasiparticle peak at the Fermi level, for the respective low-volume α-phases of the two materials. For LaTiO$_3$, a metal close to a Mott transition, LDA+DMFT calculations employing the IPT and NCA approximations to solve the DMFT equation have been compared to the more rigorous QMC [16] treatment and quantitative differences have been reported [17].

In order to analyze the Ce volume collapse, the present paper reports the first LDA+DMFT(QMC) calculations of the Ce total energy, investigating a wide range of volume and temperature. We find the low-temperature total energy to exhibit a distinctive feature which is consistent with the observed Ce volume collapse. Additional calculations of the spectral function, imaginary time Green's function, and double occupancy show that the energy feature coincides with the rapid growth of both the quasiparticle peak and the double occupancy. All these signatures moderate with increasing temperature. To provide insight into the modified local-density methods, we also contrast these LDA+DMFT(QMC) results with Hartree-Fock (HF) or static mean field solutions of the same Hamiltonians.

The DMFT(QMC) calculations in this paper solve the Hamiltonians

$$\begin{aligned} H = & \sum_{\mathbf{k},lm,l'm',\sigma} (H^0_{\rm LDA}(\mathbf{k}))_{lm,l'm'}\, \hat{c}^\dagger_{\mathbf{k}\,lm\sigma}\hat{c}_{\mathbf{k}\,l'm'\sigma} \\ & + \frac{1}{2} U_f \sum_{i,m\sigma,m'\sigma'}{}' \hat{n}_{ifm\sigma}\,\hat{n}_{ifm'\sigma'}\,, \end{aligned} \tag{1}$$

where $\mathbf{k}$ are Brillouin zone vectors, i are lattice sites, lm denote the angular momentum, σ is the spin quantum number, $\hat{n}_{ifm\sigma} \equiv \hat{c}^\dagger_{ifm\sigma}\hat{c}_{ifm\sigma}$, and the prime signifies $m\sigma \neq m'\sigma'$. The 16×16 matrices $H^0_{\rm LDA}(\mathbf{k})$ denote the matrix elements of the LDA Hamiltonian w.r.t. the 16 orbitals $(6s, 6p, 5d, 4f)$ for fcc Ce, as described in Sec. 4.2 of Ref. [2]. The $4f$ site energies are shifted to avoid double counting of the $4f$-$4f$ Coulomb interaction which is explicitly incorporated in Eq.(1) via the U_f term. These shifted site energies and the screened $4f$-$4f$ Coulomb interactions U_f were obtained by companion constrained-occupation calculations, and their values together with the effective $4f$ electron bandwidth are shown in Fig. 5 of Ref. [2] as a function of volume. Since the $4f$-orbitals are well localized, uncertainties in U_f and the $4f$ site energies are relatively small, and, given the significant volume-dependence of the $4f$ site energy, only translate into a possible volume shift. We have not included the spin-orbit interaction which has a rather small impact on LDA results for Ce, nor the intra-atomic exchange interaction which is less relevant for Ce as occupations with more than one $4f$-electron on the same site are rare.

For the present paramagnetic calculations we take the $4f$ self-energy matrix to be diagonal $\Sigma(i\omega)\,\delta_{m\sigma,m'\sigma'}$ and use two complementary approaches to perform the transformation from $G(\tau)$ to $G(i\omega_n)$. The approach described in [18] is used on a volume subgrid to validate a new faster approach which fits the $G(\tau)$ data with basis functions of the form $e^{-\tau\epsilon_i}/(e^{-\epsilon_i/T}+1)$ and which is employed for the full temperature and volume grid. Unless noted otherwise, our results are all extrapolated to the limit of zero imaginary time discretization $\Delta\tau \to 0$ in the QMC. The DMFT energy per site was evaluated from

$$E_{\rm DMFT} = \frac{T}{N}\sum_{n\mathbf{k}\sigma} {\rm Tr}(H^0_{\rm LDA}(\mathbf{k})G_{\mathbf{k}}(i\omega_n))e^{i\omega_n 0^+} + U_f\, d. \tag{2}$$

Here, Tr denotes the trace over the 16×16 matrices, T the temperature, N the number of $\mathbf{k}$ points, and

$$d = \frac{1}{2}\sum\nolimits'_{m\sigma,m'\sigma'} \langle \hat{n}_{ifm\sigma}\,\hat{n}_{ifm'\sigma'}\rangle \tag{3}$$

is a generalization of the one-band double occupation for multi-band models, calculated directly in the QMC and related to the local magnetic moment via $\langle {m_Z}^2 \rangle = \sum_{m\sigma}\langle \hat{n}_{ifm\sigma}\rangle - (2/13)\,d$.

Fig. 1a shows our calculated DMFT(QMC) energies $E_{\rm DMFT}$ as a function of atomic volume at three temperatures *relative* to the paramagnetic HF energies $E_{\rm PMHF}$ of Eq.(1), i.e., the energy contribution due to electronic correlations. Similarly given are the polarized HF energies which reproduce $E_{\rm DMFT}$ at large volumes and low temperatures. With decreasing volume, however, the DMFT energies bend away from the polarized HF solutions. This striking effect becomes more pronounced, and begins at slightly larger volume, as temperature is decreased. At $T = 0.054\,$eV, a region of negative curvature in $E_{\rm DMFT} - E_{\rm PMHF}$ is evident within the observed two phase region (arrows).

Fig. 1b presents the calculated LDA+DMFT total energy $E_{\rm tot}(T) = E_{\rm LDA}(T) + E_{\rm DMFT}(T) - E_{\rm mLDA}(T)$ where $E_{\rm mLDA}$ is the energy of an LDA-like solution of the model Hamiltonian in Eq.(1) [19]. Since both $E_{\rm LDA}$ and $E_{\rm PMHF} - E_{\rm mLDA}$ have positive curvature throughout the volume range considered, it is the negative curvature of the correlation energy in Fig. 1a which leads to the dramatic depression of the LDA+DMFT total energies in the range $V = 26$–28 Å^3 for decreasing temperature, which contrasts to the smaller changes near $V = 34$ Å^3 in Fig. 1b. This trend is consistent with a double well structure emerging at still lower temperatures (prohibitively expensive for QMC simulations), and with it the concomitant volume collapse transition. The general shallowness of our $T = 0.054\,$eV$= 632\,$K isotherm in Fig. 1b is consistent with the $\sim$550 K critical end point for the α-γ transition, as is the width of this region compared to the indicated room temperature volumes of the α and γ phases. We estimate entropy corrections TS would alter the shape of this curve by less that 0.1 eV. Furthermore, pressure-volume results (not shown) obtained from smoothed fits to our 632-K energies yield 70-110% of the observed 9.6 Å^3 change in atomic volume between γ- and α-phases at 0 and 5 GPa, respectively, and they track the experimental isotherm to within 2 and in some cases 1 Å^3 from 5 to 50 GPa. Altogether, this is reasonable agreement with experiment given our use of energies rather than free energies, the different temperatures, and the LDA and DMFT approximations.

To clarify the physical origin of the sharp energy feature, we employ the maximum entropy method to study the evolution of the $4f$ spectral function $A(\omega)$ with atomic volume. At $V = 20$ Å^3, Fig. 2 shows that almost the entire spectral weight lies in a large quasiparticle peak with a center of gravity slightly above the chemical potential. This is similar to the LDA solution, however, a weak upper Hubbard band is also present even at this small volume. At the volumes 29 Å^3 and 34 Å^3 which approximately bracket the α-γ transition, the spectrum has

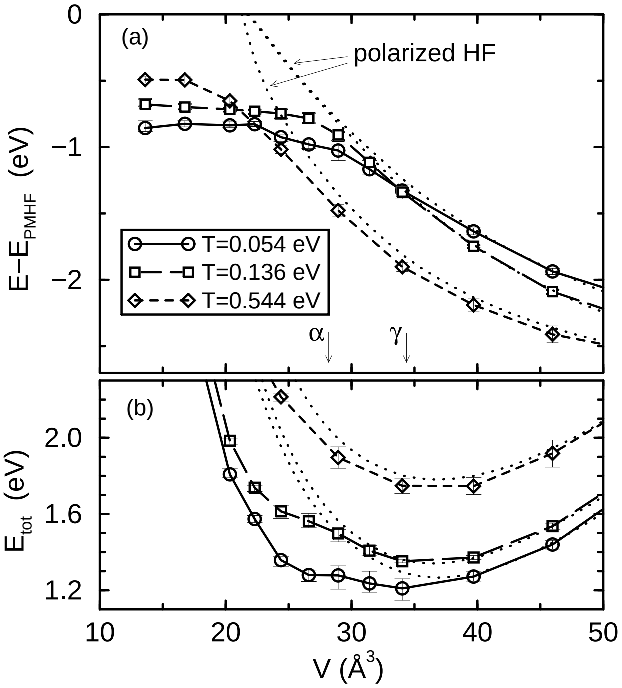

FIG. 1. (a) Correlation energy $E_{\rm DMFT}-E_{\rm PMHF}$ as a function of atomic volume (symbols) and polarized HF energy $E_{\rm AFHF}-E_{\rm PMHF}$ (dotted lines which, at large V, approach the DMFT curves for the respective temperatures); arrows: observed volume collapse from the α- to the γ-phase. The correlation energy sharply bends away from the polarized HF energy in the region of the transition. (b) The resultant negative curvature leads to a growing depression of the total energy near $V=26$–28 Å^3 as temperature is decreased, consistent with an emerging double well at still lower tempertures and thus the α-γ transition. The curves at $T=0.544$ eV were shifted downwards by -0.5 eV to match the energy range.

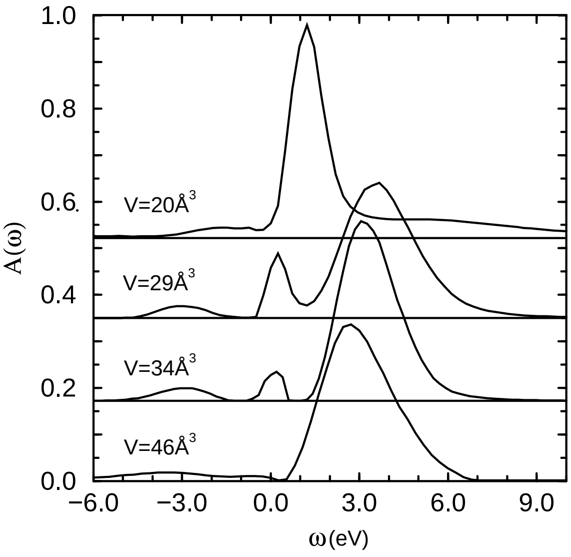

FIG. 2. Evolution of the $4f$ spectral function $A(\omega)$ with volume at $T=0.136$ eV ($\omega=0$ corresponds to the chemical potential; curves are offset as indicated; $\Delta\tau=0.11$ eV^{-1}). Coinciding with the sharp anomaly in the correlation energy (Fig. 1), the central quasiparticle resonance disappears.

a three peak structure which consists of a quasiparticle peak or Abriksov-Suhl resonance at the Fermi energy, in addition to the two Hubbard side bands at about ±3 eV. The quasiparticle peak is seen to dramatically shrink in going from $V=29$ Å^3 to $V=34$ Å^3, which coincides with the range of negative curvature in the correlation energy. Finally, by $V=46$ Å^3, the central peak has disappeared leaving only the lower and upper Hubbard bands in the spectrum.

An alternative quantity that allows the study of the spectrum close to the Fermi energy is the Green function at imaginary time $\tau=\beta/2$, since in the limit of low temperature the density of states at the Fermi level is given by $N(0)=-(\beta/\pi)\,G(\beta/2)$ [20]. With increasing volume, the low-temperature results in Fig. 3a show first an increase in the quasiparticle peak around the chemical potential due to narrowing of the LDA $4f$-bands, followed by a sharp drop at the α-γ transition, supporting the results of Fig. 2.

To measure the itinerant or localized character we study the generalized double occupancy d of Eq. (3). For fully localized spins, d takes its smallest value at the minimal fraction of sites having two $4f$-electrons which is $d_{min}=\max(0,n_f-1)$ for $n_f\leq 2$. In contrast, for a fully itinerant system in the uncorrelated U_f=0 limit, the maximal value $d_{max}=(13/28)n_f^2$ is obtained, corresponding to $\langle n_{m\sigma}n_{m'\sigma'}\rangle=(n_f/14)^2$. With decreasing volume, Fig. 3b clearly shows a dramatic increase in the ratio $(d-d_{min})/(d_{max}-d_{min})$ associated to the onset of delocalization. However, the delocalization is not completed and d is still considerably lower than its maximal value, even at the lowest volumes of Fig. 3b. This reflects the correlated nature of the α-phase with a reduced Coulomb interaction energy $U_f\,d$ and thus, compared to the uncorrelated static mean field solution, a lower DMFT energy in Fig. 1a. The rapid increase in double occupancy implies that the local magnetic moment shows a considerable change at the transition (the increase for small volumes is due to an increase in n_f) which is, however, less pronounced than in the static mean field theories.

In conclusion, our LDA+DMFT(QMC) calculations for Ce show an anomaly in the correlation energy leading to a shallowness in the total energy close to the critical endpoint for the α-γ transition, and suggest an emerging double well as temperature is further decreased, consistent with the observed transition. The $4f$-spectra and a measure of the $4f$-spectrum at the Fermi level show Hubbard splitting in the large-volume γ-phase, with an Abrikosov-Suhl-like quasiparticle peak first appearing at the Fermi level in the transition region, and then growing at the expense of the Hubbard side-bands with subsequent compression in the α-phase. These are characteristic attributes of the Kondo volume collapse picture for Ce [3]. On the other hand, we also find a rapid increase in

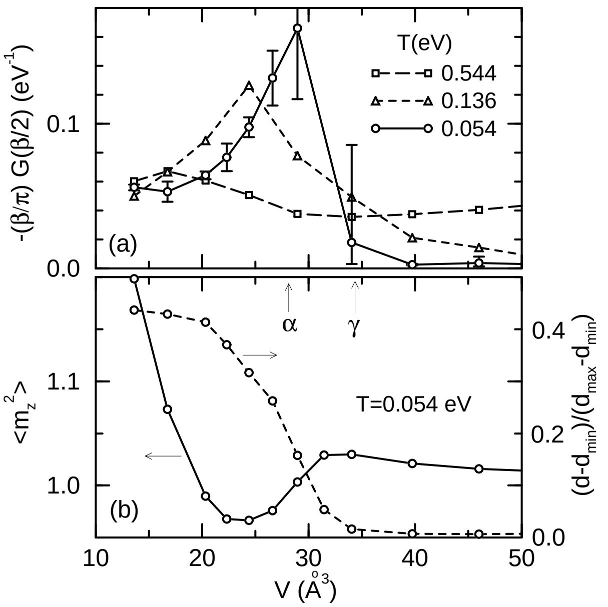

FIG. 3. (a) $-(\beta/\pi)\,G(\beta/2)$ vs. volume, which at low temperature gives the $4f$ spectral weight at the chemical potential; (b) Local magnetic moment and ratio of the double occupancy vs. volume. The latter indicates that the γ-α transition coincides with the onset of delocalization.

the double occupancy at low temperature in going from the γ- to the α-phases, which could be interpreted as increased itinerancy of the $4f$-electrons, a tenet of the Mott transition picture [4]. There may well be greater similarities between the two scenarios than has been accepted, as argued recently in a comparison of many-body solutions of the respective Anderson and Hubbard model paradigms for these pictures [21].

Our comparison of HF to the DMFT energies also offers insight into the modified local-density calculations for the Ce transition [6,7,22], which resemble static mean field treatments. Our results suggest that polarized solutions can give good low-temperature energies at large volume for the γ-phase, however, may be offset in energy in the low-volume paramagnetic α-regime. Even so, it is tempting to speculate from Fig. 1a that their slopes are correct, which would reconcile standard LDA or generalized gradient extensions [23] doing so well for the volume dependence in the itinerant phases, even though they can not capture the residual Hubbard splitting.

We acknowledge support by the Alexander von Humboldt foundation (KH) and NSF-DMR-9985978 (RTS). Work by AKM was performed under the auspices of the U.S. DOE by U. Cal., LLNL under contract No. W-7405-Eng-48. We are grateful for the QMC code of [8] (App. D) which was modified for use in part of the present work, to A. Sandvik for making available his maximum entropy code, and to D. Vollhardt and G. Esirgen for useful discussions.

[1] *Handbook on the Physics and Chemistry of Rare Earths*, edited by K. A. Gschneider Jr. and L. R. Eyring (North-Holland, Amsterdam, 1978); in particular, D. G. Koskenmaki and K. A. Gschneider Jr., *ibid*, p.337.

[2] A. K. McMahan *et al.*, J. Comput.-Aided Mater. Design **5**, 131 (1998).

[3] J. W. Allen and R. M. Martin, Phys. Rev. Lett. **49**, 1106, (1982); J. W. Allen and L. Z. Liu, Phys. Rev. B **46**, 5047, (1992); M. Lavagna, C. Lacroix, and M. Cyrot, Phys. Lett. **90A**, 210 (1982).

[4] B. Johansson, Philos. Mag. **30**, 469 (1974); B. Johansson *et al.*, Phys. Rev. Lett. **74**, 2335 (1995).

[5] C. Huscroft *et al.*, Phys. Rev. Lett. **82**, 2342 (1999).

[6] O. Eriksson, M. S. S. Brooks, and B. Johansson, Phys. Rev. B **41**, 7311 (1990).

[7] A. Svane *et al.*, Phys. Rev. B **56**, 7143 (1997); Z. Szotek *et al.*, Phys. Rev. Lett. **72**, 1244 (1994); A. Svane, Phys. Rev. Lett. **72**, 1248 (1994).

[8] A. Georges *et al.*, Rev. Mod. Phys. **68**, 13 (1996).

[9] F. Gebhard, *The Mott Metal-Insulator Transition* (Springer, Berlin, 1997).

[10] V. I. Anisimov *et al.*, J. Phys. Cond. Matter **9**, 7359 (1997); A. I. Lichtenstein and M. I. Katsnelson, Phys. Rev. B **57**, 6884 (1998); for an introduction, see K. Held *et al.*, preprint cond-mat/0010395.

[11] See, e.g., R. O. Jones and O. Gunnarsson, Rev. Mod. Phys. **61**, 689 (1989).

[12] D. Vollhardt, in *Correlated Electron Systems*, edited by V. J. Emery (World Scientific, Singapore) 57 (1993); Th. Pruschke, M. Jarrell, and J. K. Freericks, Adv. Phys. **44**, 187 (1995).

[13] For Ce, intersite correlations are less important since the Coulomb interaction is between well localized $4f$-electrons and the volume collapse transitions occur at room temperature well above any magnetic order.

[14] S. Y. Savrasov, G. Kotliar, and E. Abrahams, Nature **410**, 793 (2001); preprint, cond-mat/0106308.

[15] M. B. Zölfl *et al.*, preprint, cond-mat/0101280.

[16] For one-band DMFT(QMC) see [8] and M. Jarrell, in *Numerical Methods for Lattice Quantum Many-Body Problems*, editor D. Scalapino (Addison Wesley, 1997).

[17] I. A. Nekrasov *et al.*, Eur. Phys. J. B **18**, 55 (2000).

[18] For details of the algorithm, see M. Ulmke, V. Janiš, and D. Vollhardt, Phys. Rev. B **51**, 10411 (1995).

[19] We solve self-consistently for n_f using a $4f$ self energy $\Sigma = U_f(n_f - \frac{1}{2})$, and then remove this contribution from the eigenvalue sum to get the kinetic energy. The potential energy is taken to be $\frac{1}{2}U_f n_f(n_f - 1)$.

[20] N. Trivedi and M. Randeria, Phys. Rev. Lett. **75**, 312 (1999).

[21] K. Held *et al.*, Phys. Rev. Lett. **85**, 373 (2000); K. Held and R. Bulla, Eur. Phys. J. B **17**, 7 (2000).

[22] A. B. Shick, W. E. Pickett, and A. I. Liechtenstein, cond-mat/0001255.

[23] P. Söderlind, Adv. Phys. **47**, 959 (1998).